Available online at www.sciencedirect.com
ScienceDirect
Trans. Nonferrous Met. Soc. China 28(2018) 1157−1165
Transactions of Nonferrous Metals Society of China
www.tnmsc.cn

Glass formation, thermal and mechanical properties of ZrCuAlNi bulk metallic glasses

C. E. BORJA[1], I. A. FIGUEROA[2], O. LOZADA-FLORES[2], M. ESTRADA[2], G. A. LARA-RODRÍGUEZ[2], J. A. VERDUZCO[1]

1. Instituto de Investigación en Metalurgia y Materiales, Universidad Michoacana de San Nicolás de Hidalgo (UMSNH), Fco. J. Mújica S/N, Col. Felícitas del Río, C.P. 58030, Morelia, Mich., México;
2. Instituto de Investigaciones en Materiales, Universidad Nacional Autónoma de México (UNAM), Circuito Exterior S/N, Cd. Universitaria, C.P. 04510, Cd. Mx., México

Received 20 April 2017; accepted 28 September 2017

Abstract: The glass forming ability, thermal and mechanical properties of some ZrCuAlNi bulk metallic glasses were analyzed. The compositions of the alloys were theoretically determined with the dense packing and kinetic fragility index models. Cylindrical and conical ingots were produced by copper mould suction-casting under Ar atmosphere. The conical ingots were characterized by means of X-ray diffraction in order to determine the glassy structure. It was found that both alloys have a critical glassy diameter, D_c, of 3 mm. Thermal behaviours were investigated by differential scanning calorimetry at heating rates of 0.5, 0.67 and 0.83 K/s. The gamma parameter γ, supercooled liquid region ΔT_x, and reduced glass transition temperature T_{rg}, of the experimentally obtained glasses indicated high glass forming ability. The glassy compositions showed a fragility index of ~40 GPa. The compression test of the investigated alloys was carried out at a strain rate of 0.016 s^{-1}, obtaining a elastic modulus of ~83 GPa, total deformation of ~5%, yield strength of 1.6 GPa and hardness of 4 GPa. It was concluded that the use of the dense packing and kinetic fragility index models helped to predict glass-forming compositions in the family alloy investigated.
Key words: bulk metallic glass; glass formation ability; fragility index; packing efficiency; suction casting

1 Introduction

Bulk metallic glasses (BMGs), are interesting metallic materials, as they have shown exceptional properties or combination of properties that are often not achievable by their conventional crystalline counterparts [1]. The Zr-based bulk metallic glasses have excellent mechanical properties, elastic modulus (E ~80 GPa), and tensile strength (σ_y ~1.5 GPa). The excellent mechanical properties of Zr-based BMGs have been exploited commercially in golf clubs, followed by tennis rackets, baseball and softball bats, skis and snowboards, bicycle parts, scuba gear, etc. [2] Besides, various Zr-based BMGs have demonstrated potential for biomedical applications [2,3].

Many criteria have been used to describe the glass-forming ability (GFA). For example, the critical glassy diameter parameter (D_c) which is directly proportional to the GFA. The D_c corresponds to the maximum thickness of an alloy with glassy structure. In order to explain the glass formation and thermal stability of the glasses, these criteria have been based on the transformation temperature. Some of the most used thermally obtained parameter are the gamma parameter, $\gamma=T_x/(T_g+T_x)$, supercooled liquid region, $\Delta T_x=(T_x-T_g)$, and reduced glass transition temperature, $T_{rg}=T_g/T_l$, where T_x, T_g and T_l represent the crystallization, glass-transition and liquid temperatures, respectively. However, these parameters can only be determined from previously obtained glasses [2,4], and therefore, are called “post-morten”. On the other hand, topological models have been proposed in order to describe the glass formation, for example, the dense packing model. This model includes the calculation of the three-dimensional coordination number N^T, which is obtained for a radius ratio, R^*, for maximum packing efficiency. The chemical compositions were calculated based on a sphere-packing

Corresponding author: I. A. FIGUEROA; E-mail: iafigueroa@unam.mx
DOI: 10.1016/S1003-6326(18)64753-3

scheme (solute-centred clusters occupying an fcc cluster unit cell). The packing efficiency is calculated from the chemical composition and cluster unit cell length of the alloy [5−7].

ANGELL et al [8,9] introduced the concept of fragility, which is defined as the increasing rate of the viscosity of a supercooled liquid at the glass transition temperature, during the cooling process. The term fragility (m), was proposed as a good indicator of glass formation. The magnitude of m, is defined in terms of the shear viscosity, as

$$m=\left.\frac{\partial \lg T}{\partial \lg(T_g/T)}\right|_{T=T_g} \tag{1}$$

Therefore, m is an index that shows how fast the viscosity increases while approaching the structural arrest at T_g, the temperature at which the viscosity is 1×10^{12} Pa·s [10]. The kinetic fragility index was used as a glass forming parameter, being also calculated as follows [11]:

$$m=12(K/G+0.67) \tag{2}$$

where K is the bulk modulus (GPa) and G is the shear modulus (GPa).

From the resulting value of m, the glass-forming liquids were originally classified as strong and fragile liquids. The top and bottom values of such parameter were estimated between 16 substances, which were considered strong (high GFA) and 200 for fragile systems with low GFA.

The topological model of densely packed clusters and the fragility index, have been used in the design of BMG in quaternary alloy systems [12]. Based on these models, several ZrCuAlNi alloys were calculated. The compositions with higher packing efficiency were experimentally investigated. In this work, the GFA of some Zr-based alloys is explained in terms of the topological model of densely packed clusters, fragility index, critical diameter and thermal parameters. In addition, the microstructural and mechanical properties of the investigated glassy alloys were assessed.

2 Theoretical calculation and experimental procedure

2.1 Theoretical chemical composition calculation

The chemical compositions of the ZrCuAlNi system were calculated using the topological model of densely packed clusters [5−7]. First, the calculations of atomic radii ratios, $R=r_i/r_\Omega$, between the solute atoms, r_i ($i=\alpha$, β and γ) and solvent atoms, r_Ω, were carried out. Depending on the R value, the number of coordination, N^T, was calculated using Eqs. (3−5) [6]:

$$N^T=\frac{4\pi}{6\arccos\left(\sin\left(\frac{\pi}{3}\right)\left[1-\frac{1}{(R+1)^2}\right]^{1/2}\right)-\pi},\quad 0.225\le R<0.414 \tag{3}$$

$$N^T=\frac{4\pi}{8\arccos\left(\sin\left(\frac{\pi}{4}\right)\left[1-\frac{1}{(R+1)^2}\right]^{1/2}\right)-2\pi},\quad 0.414\le R<0.902 \tag{4}$$

$$N^T=\frac{4\pi}{10\arccos\left(\sin\left(\frac{\pi}{5}\right)\left[1-\frac{1}{(R+1)^2}\right]^{1/2}\right)-3\pi},\quad 0.902\le R \tag{5}$$

For the quaternary system, it was considered that each atomic specie was accommodated in its corresponding place of the fcc cell clusters. Therefore, the number of solvent atoms, N_Ω, was calculated as follows [5]:

$$N_\Omega=\frac{N_\alpha}{1+12/N_\alpha} \tag{6}$$

where N_α is the number of coordination calculated with Eq. (4).

The chemical composition was obtained with the total number of atoms resulting from the sum of $N_\Omega+1\alpha+1\beta+2\gamma$, since in the fcc packing, there are 1β site and 2γ sites for each α site [5]. The α and β concentrations are the same and it is possible to obtain several chemical compositions, considering different positions of the solute atoms in the cluster cell.

2.1.1 Packing efficiency calculation

In order to determine the cell cluster volume (V_{cell}) for each calculated composition, Eqs. (7)−(9) were used [5]. The distances of $d_{\langle100\rangle}$, $d_{\langle110\rangle}$ and $d_{\langle111\rangle}$ were compared and the distance of greater magnitude (Λ_o) was used to calculate the cell cluster volume (Λ_o^3).

$$d_{\langle100\rangle}=2r_\Omega\left[\sqrt{(R_\alpha+1)^2-4/3}+\sqrt{(R_\beta+1)^2-4/3}\right] \tag{7}$$

$$d_{\langle110\rangle}=4r_\Omega\left[\sqrt{(R_\alpha+1)^2-4/3}\right] \tag{8}$$

$$d_{\langle111\rangle}=2r_\Omega\left[\sqrt{(R_\alpha+1)^2-4/3}+\sqrt{(R_\beta+1)^2-4/3}+\sqrt{(R_\gamma+1)^2-4/3}\right] \tag{9}$$

where R_α, R_β and R_γ are atomic radii ratios of r_i/r_Ω, $i=\alpha$, β and γ.

Since the packaging efficiency value, η, could be directly proportional to the glass forming ability, η is calculated as follows:

$$\eta = \frac{V_{at}}{V_{cell}} \quad (10)$$

where V_{at} is the volume of the atoms in the fcc cluster cell and V_{cell} is the volume occupied by the cell clusters.

2.1.2 Fragility index calculation

The fragility index for the calculated composition was obtained with Eq. (2). The bulk modulus K (GPa) and shear modulus G (GPa) were determined with the "rule of mixtures" [10] and finally, the calculated compositions were classified according to the resulted m values, obtained from the same equation.

2.2 Experimental procedure

The alloy ingots were prepared from elemental metals of pure Zr, Al, Ni, Cu (purity >99.8%) by arc-melting, under a Ti gettered Ar atmosphere. The ingots were re-melted five times to ensure chemical homogeneity. The alloy compositions represent the nominal values since the mass loss in melting was negligible (<0.1%). Conical alloy ingots of 30 mm in length, with a minimum diameter of 1 mm and maximum diameter of 8 mm, were produced by copper mould suction-casting within the argon arc furnace. Similarly, ingots of 2 mm in diameter and 37 mm in length were produced. The conical ingots were cut crosswise in 3 and 4 mm of diameter and verified by X-ray diffractometry by means of a Siemens D5000 diffractometer using Cu K_α radiation to determine the critical glassy diameter, D_c. Cylindrical samples were used for hardness and compression test. The compression test was carried out at a strain rate of 0.016 s^{-1}, using a Zwick Roell testing machine at room temperature. The scanning electron microscopy (SEM), JEOL JMS 600 equipped with an energy dispersive X-ray spectrometer EDX, was used for elemental mapping (chemical homogeneity) and microstructural analysis. The thermal behaviour was investigated by means of a TA instruments SDT-Q600 differential scanning calorimeter, with an Ar flow and heating rates of 0.5, 0.67 and 0.83 K/s.

3 Results and discussion

3.1 Glass-forming ability

The $Zr_{52.3}Cu_{23.9}Al_{11.9}Ni_{11.9}$ and $Zr_{57.2}Cu_{21.4}Al_{10.7}Ni_{10.7}$ compositions were calculated by means of the dense packing model [5−7]. Table 1 shows the calculated chemical compositions with the topological model. The packing efficiency changed as a function of the central positions of the clusters α, β, γ and Ω. According to the model, the atomic concentration is approximately 60% γ, 10% α, 10% β and 20% Ω [5]. Therefore, it is worth noting that the chemical compositions shown in Table 1 were obtained at intercalating positions, in the clusters cells, of the aforementioned solute elements (i.e., γ, α, β and Ω). The values of Λ_o^3, η and m were also calculated for the investigated chemical compositions. The magnitude of these parameters was strongly related to the atomic size of the involved chemical elements and the solute atom positions. On the other hand, the K/G elastic constant relation also influences the value of m.

Table 1 Calculated values of packing efficiency η and fragility index m for Zr−Al−Ni−Cu system

Chemical composition	η/%	m
$Zr_{57.2}Ni_{21.4}Al_{10.7}Cu_{10.7}$	46.98	39.7
$Zr_{57.2}Cu_{21.4}Al_{10.7}Ni_{10.7}$	46.56	40.8
$Zr_{53.1}Ni_{23.5}Al_{11.7}Cu_{11.7}$	41.91	39.6
$Zr_{52.3}Cu_{23.9}Al_{11.9}Ni_{11.9}$	40.57	40.8
$Zr_{53.1}Al_{23.5}Ni_{11.7}Cu_{11.7}$	40.13	40.7
$Zr_{52.3}Al_{23.9}Ni_{11.9}Cu_{11.9}$	39.21	40.6

The packing efficiency and chemical compositions of the $Zr_{57.2}Ni_{21.4}Al_{10.7}Cu_{10.7}$ (46.98%) and $Zr_{57.2}Cu_{21.4}Al_{10.7}Ni_{10.7}$ (46.56%) are rather similar, thus their GFA is expected to be also akin. However, in order to improve the cooling rate in the solidification process, since the heat transfer index, k, of Cu (398 W/(m·K) is higher than those Al and Ni (237 and 91 W/(m·K), respectively) [13], the $Zr_{57.2}Cu_{21.4}Al_{10.7}Ni_{10.7}$ and $Zr_{52.3}Cu_{23.9}Al_{11.9}Ni_{11.9}$ compositions were selected for experimental validation. The fragility index value of the chosen $Zr_{57.2}Cu_{21.4}Al_{10.7}Ni_{10.7}$ and $Zr_{52.3}Cu_{23.9}Al_{11.9}Ni_{11.9}$ compositions was 40.8, also indicating the possibility to form a glassy phase for both alloys.

Figure 1 shows the conical and cylindrical ingots obtained by the suction casting technique. The suction casting technique is normally used in order to obtain a glassy phase in bulk shapes (>1 mm in diameter), which

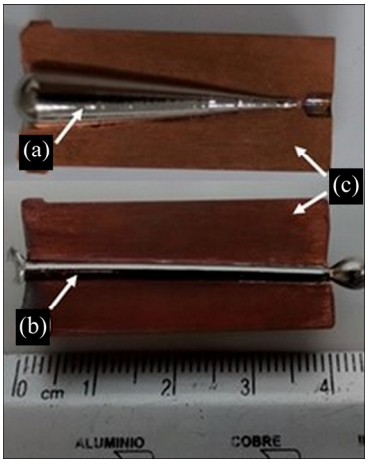

Fig. 1 Conical and cylindrical ingots obtained from suction casting: (a) Conical sample; (b) Cylindrical sample; (c) Cu mould

has been extensively used [14−17]. The ingots showed a metallic lustre, which indicated that the preparation process did prevent the oxidation of the alloys. The cylindrical bars were useful for the mechanical testing and the conical ingots were taken for the critical glassy diameter analysis.

Figure 2 shows the XRD patterns of the studied alloys, with a cross-section diameter of 3 mm. Both alloys displayed a diffuse diffraction pattern localized between 2θ of 30° and 50° without a detectable sharp Bragg peak. Therefore, these alloys can be considered as BMGs with a critical glassy diameter, D_c, of 3 mm. It also confirms the usefulness of the theoretical models used in this work to design bulk metallic glasses in the studied system.

Figure 3 displays the X-ray diffraction patterns of the same alloys, but now, for samples with a cross-section diameter of 4 mm, the patterns showed the presence of sharp peaks in 2θ of 30°−100°, which indicates that these alloys have a partly crystalline structure. It is worth mentioning that the amount of glassy phase dropped considerably, i.e. from a fully glassy phase (Fig. 2) to a 20% glassy−80% crystalline structure.

Figure 4 shows the elemental EDS mapping taken from the scanning electron microscope. The EDS analysis results indicated the chemical homogeneity of the $Zr_{57.2}Cu_{21.4}Al_{10.7}Ni_{10.7}$ alloy. It is also evident that no atomic segregation was found, the mapping showed a homogeneous atomic distribution in the as-cast bulk metallic sample. It is worth mentioning that the chemical

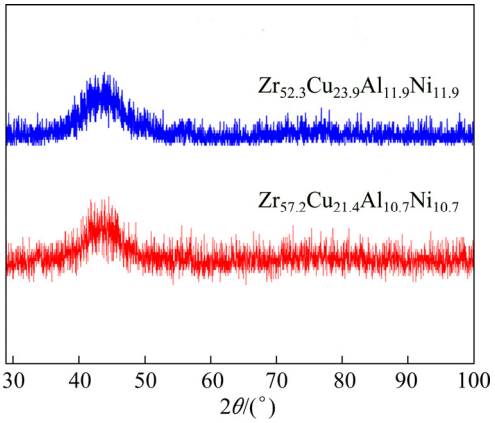

Fig. 2 XRD patterns of studied ZrCuAlNi alloys with cross-section diameter of 3 mm

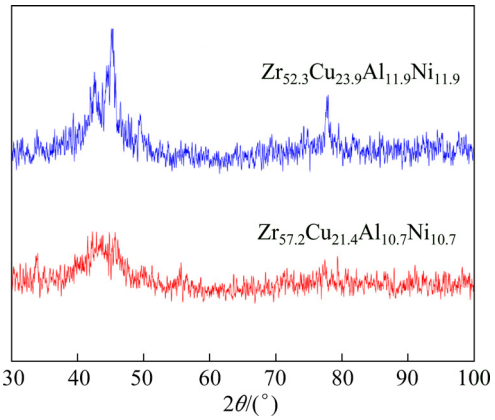

Fig. 3 XRD patterns of ZrCuAlNi alloys with cross-section diameter of 4 mm

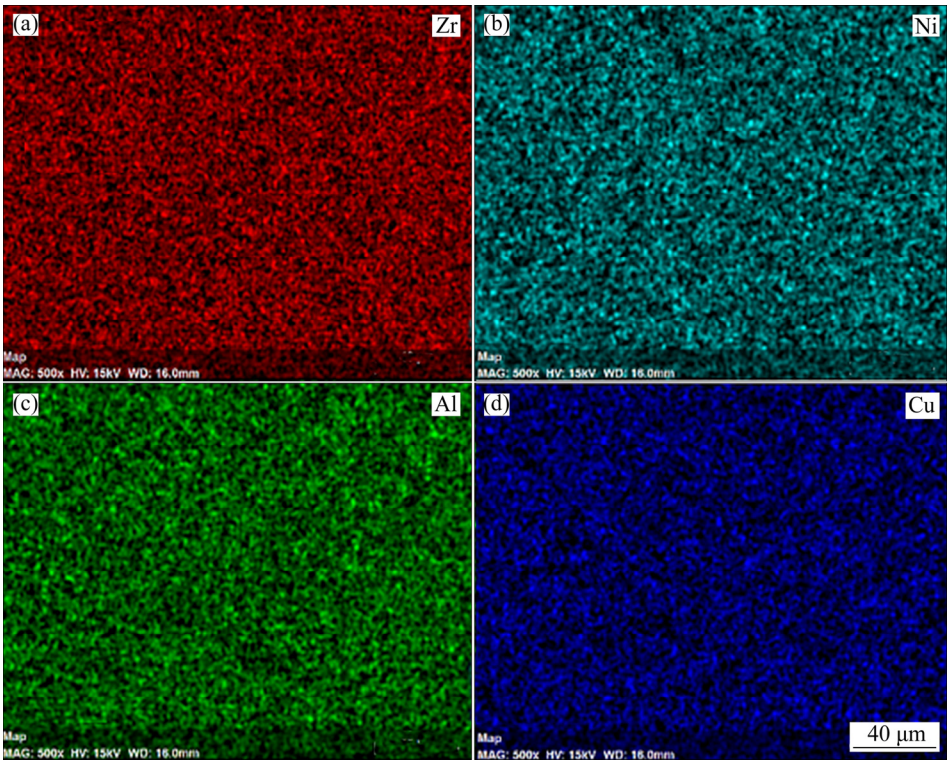

Fig. 4 Chemical mapping of $Zr_{57.2}Cu_{21.4}Al_{10.7}Ni_{10.7}$ glassy alloy

homogeneity was identical for both, experimentally obtained, Zr-based alloys.

Figures 5 and 6 show the DTA thermograms of the $Zr_{57.2}Cu_{21.4}Al_{10.7}Ni_{10.7}$ and $Zr_{52.3}Cu_{23.9}Al_{11.9}Ni_{11.9}$ glasses at different heating rates. The peak intensity and transformation temperatures, such as glass transition T_g, crystallization T_x, solidus T_m and liquidus T_l, varied with respect to the heating rate v.

Table 2 summarizes the transformation temperatures from the differential thermal analysis curves shown in Figs. 5−6, and also includes the GFA thermal parameters of the experimentally produced glassy alloys. The magnitude of ΔT_x for the $Zr_{57.2}Cu_{21.4}Al_{10.7}Ni_{10.7}$ is slightly higher than that for the $Zr_{52.3}Cu_{23.9}Al_{11.9}Ni_{11.9}$ alloy at different heating rates. Although the ΔT_x difference is minimal, the η plays an important role in the magnitude of this parameter, i.e., as the η increases the atomic diffusion decreases, affecting the magnitude of the supercooled liquid region.

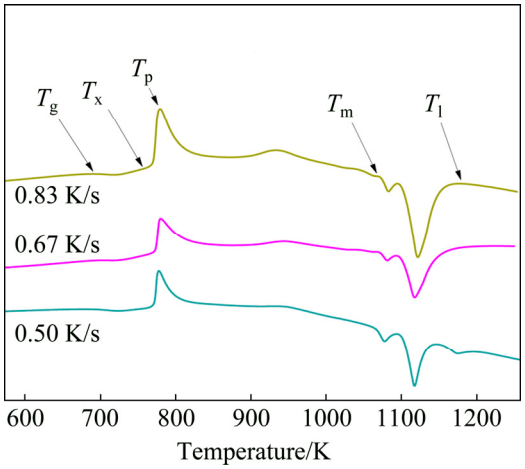

Fig. 5 Thermal analysis of $Zr_{57.2}Cu_{21.4}Al_{10.7}Ni_{10.7}$ alloy at different heat rates

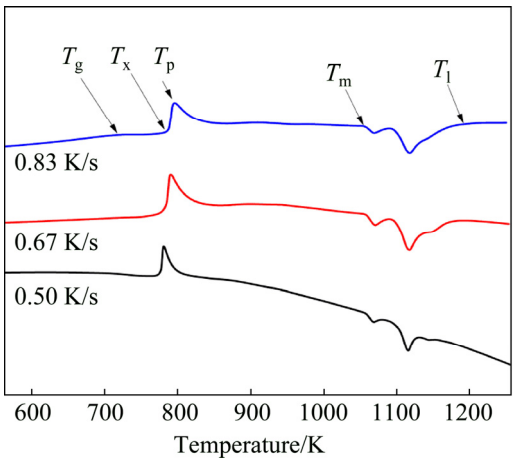

Fig. 6 Calorimetric analysis of $Zr_{52.3}Cu_{23.9}Al_{11.9}Ni_{11.9}$ alloy at different heat rates

The transformation temperatures for the $Zr_{57.2}Cu_{21.4}Al_{10.7}Ni_{10.7}$ and $Zr_{52.3}Cu_{23.9}Al_{11.9}Ni_{11.9}$ glasses at a heating rate of 0.67 K/s were similar to that for Zr−Al−Ni−Cu at the same heating rate [16]. Regarding to T_{rg}>0.66 [2], it is suggested that at T_{rg}>0.66, the homogeneous nucleation of the crystalline phase is completely suppressed. Most typically, a minimum value of $T_{rg}\cong 0.4$ has been found to be necessary for an alloy to become a glass, but the higher the T_{rg} value is, the easier it is to form a glassy phase [2]. The average T_{rg} values of $Zr_{57.2}Cu_{21.4}Al_{10.7}Ni_{10.7}$ and $Zr_{52.3}Cu_{23.9}Al_{11.9}Ni_{11.9}$ were 0.62 and 0.65, respectively, matching with T_{rg} criterion. According to γ parameter, BMGs can be obtained with γ>0.35, which is consistent with the γ values experimentally obtained for the investigated glassy alloys. On the other hand, the cooling rate for glass formation in sections of 3 mm is between 770 and 885 K/s, which is higher than that for sections of 4 mm (540−620 K/s) [18], when casting in water-cooled copper moulds. This also explains the obtained vitreous structure in the investigated alloys.

According to previous reports [19], for the Zr−Al−Ni−Cu glassy system the ΔT_x and D_c values were 63.3 K and 7.5 mm for $Zr_{62.5}Al_{12.1}Cu_{7.95}Ni_{17.45}$, 68.9 K and 6.5 mm for $Zr_{63}Al_{11.4}Cu_{9.3}Ni_{16.3}$ and 71 K and 6 mm for $Zr_{63.5}Al_{10.7}Cu_{10.7}Ni_{15.1}$ glassy alloys. Although a number of alloys of this family have been reported in the literature, the glass forming ability of them has been found out after the experimental process (trial and error). However, in this work, based on theoretical models, it was possible to design and produce bulk metallic glasses beforehand, reducing the experimental work and resources, associated with standard experimental processes.

Table 2 Thermal properties and GFA thermally obtained parameters for investigated alloys

Alloy	v/(K·s^{-1})	T_g/K	T_x/K	T_m/K	T_l/K	ΔT_x/K	T_{rg}	γ
$Zr_{57.2}Cu_{21.4}Al_{10.7}Ni_{10.7}$	0.83	666	765	1067	1170	98.5	0.624	0.416
	0.67	659	763	1064	1154	104.2	0.619	0.42
	0.5	653	762	1059	1145	108.7	0.617	0.423
$Zr_{52.3}Cu_{23.9}Al_{11.9}Ni_{11.9}$	0.83	693	784	1058	1145	91.4	0.654	0.426
	0.67	689	779	1053	1143	90.6	0.654	0.425
	0.5	685	774	1047	1140	89.7	0.653	0.424

$\Delta T_x=T_x-T_g$; $T_{rg}=T_g/T_m$; $\gamma=T_x/(T_g+T_l)$

3.2 Mechanical properties

Table 3 shows the elastic properties of the calculated compositions with the dense packing model [5−7], for the ZrCuAlNi system. The elastic modulus E, shear modulus G and bulk modulus K, were calculated with "rule of mixtures". Table 3 also includes the values of the elastic constants for cubic system c_{11}, c_{12} and c_{44}. The elastic constants C_{ij} were calculated with Eqs. (11)−(13) [10].

$$c_{11}=K+(4/3)G \quad (11)$$

$$c_{12}=(3K-c_{11})/2 \quad (12)$$

$$c_{44}=G \quad (13)$$

Figure 7 shows a Blackman diagram of the theoretically calculated chemical compositions (packing model). This shows the values at the upper left (low c_{44}/c_{11} and high c_{12}/c_{11}), which indicates ductile mechanical behaviour [20]. The theoretical values of the Poisson ratio (υ) for the calculated compositions were added to the Blackman diagram. The calculated values of Poisson ratio for all compositions are higher than the critical value ($\upsilon \sim 0.32$), suggesting a ductile mechanical behaviour [10]. The Poisson ratio of the $Zr_{57.2}Cu_{21.4}Al_{10.7}Ni_{10.7}$ and $Zr_{52.3}Cu_{23.9}Al_{11.9}Ni_{11.9}$ alloys was 0.336, indicating the same mechanical behaviour.

Figure 8 shows the compressive stress−strain curves of the investigated alloys. The mechanical behaviour of both alloys was very similar, matching with the calculated Poisson ratio and Blackman criteria. The amount of plastic deformation obtained for both alloys did confirm that the theoretical calculation did match with the experimental results, as the percentage of the total deformation doubles the typical values for BMGs (<2%). Table 4 shows the mechanical properties for the BMG experimentally obtained; the hardness H, deformation ε and yield strength σ_y, were obtained at room temperature. Table 3 also includes the elastic modulus E* and hardness H^*, calculated using the $EH_v^{-1}\sim 2.5$ and $E\sigma_f^{-1}\sim 50$ relationships [10]. As mentioned above, the plastic deformation almost tripled the values of the standard metallic glasses, i.e. 5.2% and 5% for the, $Zr_{57.2}Cu_{21.4}Al_{10.7}Ni_{10.7}$ and $Zr_{52.3}Cu_{23.9}Al_{11.9}Ni_{11.9}$, respectively. The elastic modulus calculated with the "rule of mixtures" and the $E\sigma_f^{-1}\sim 50$ relationship of the $Zr_{57.2}Cu_{21.4}Al_{10.7}Ni_{10.7}$ (83.8 and 85.0 GPa) and $Zr_{52.3}Cu_{23.9}Al_{11.9}Ni_{11.9}$ (83.9 and 85.0 GPa) glasses were also similar. Serrated behaviour for both BMG was observed at the crest peaks.

According to Ref. [2], when shear bands form and propagate, a sudden drop in load is noticed in the stress−strain plot. The surrounding material recovers elastically and arrests the shear-band propagation, therefore, when this process is repeated, serrated flow behaviour is produced.

Figures 9(a)−(d) show the $Zr_{57.2}Cu_{21.4}Al_{10.7}Ni_{10.7}$ sample tested under compression load. The fracture angle of the shear plane for $Zr_{57.2}Cu_{21.4}Al_{10.7}Ni_{10.7}$ and $Zr_{52.3}Cu_{23.9}Al_{11.9}Ni_{11.9}$ glasses was ~45°, corresponding to the shear fracture mode and the phenomenon of "inhomogeneous" deformation. The shear fracture mode is typical in compression and tensile tests of BMGs, where the final fracture occurs along the shear plane, as shown in Fig. 9(b). The shear fracture mode often appears in ductile BMGs (such as those based on Zr, Cu, Ti and noble metals) [21]. Figure 9(d) shows the characteristic fracture patterns of the Zr-based metallic glasses. The vein-like patterns, river-like patterns, shear bands and smooth regions are clearly observed.

Lewandowski and Greer reported an experimental method based on a fusible coating, which showed that the temperature increases, over a few nanoseconds, during the plastic deformation [22]. This report also mentioned that such temperature increment could be as high as a few thousand Kelvin. Figure 10 shows the mechanical compression test of the $Zr_{57.2}Cu_{21.4}Al_{10.7}Ni_{10.7}$ bulk metallic glass. Here an incandescent spark was produced when the glassy samples were mechanically tested. From this, it can be assumed that the temperature increment on the fracture surface was much higher than that of the liquidus temperature for the investigated alloys, confirming the results reported in Ref. [22].

Table 3 Elastic properties of calculated composition, elastic constant and elastic constant relationship

Chemical composition	E/GPa	G/GPa	K/GPa	υ	c_{11}/GPa	c_{12}/GPa	c_{44}/GPa	c_{12}/c_{11}	c_{44}/c_{11}
$Zr_{57.2}Ni_{21.4}Al_{10.7}Cu_{10.7}$	76.1	43.1	113.7	0.3317	156.8	92.2	43.1	0.5881	0.2746
$Zr_{57.2}Cu_{21.4}Al_{10.7}Ni_{10.7}$	83.8	40.1	109.5	0.3368	149.5	89.4	40.1	0.5981	0.2679
$Zr_{53.1}Ni_{23.5}Al_{11.7}Cu_{11.7}$	75.4	37.5	106.5	0.3424	144	87.8	37.5	0.6098	0.2601
$Zr_{52.3}Cu_{23.9}Al_{11.9}Ni_{11.9}$	83.9	40.9	111.6	0.3367	152.5	91.2	40.9	0.5978	0.2681
$Zr_{53.1}Al_{23.5}Ni_{11.7}Cu_{11.7}$	90.7	38.2	103.7	0.3359	141.9	84.6	38.2	0.5966	0.269
$Zr_{52.3}Al_{23.9}Ni_{11.9}Cu_{11.9}$	90.8	38.3	103.9	0.3358	142.2	84.8	38.3	0.5965	0.269

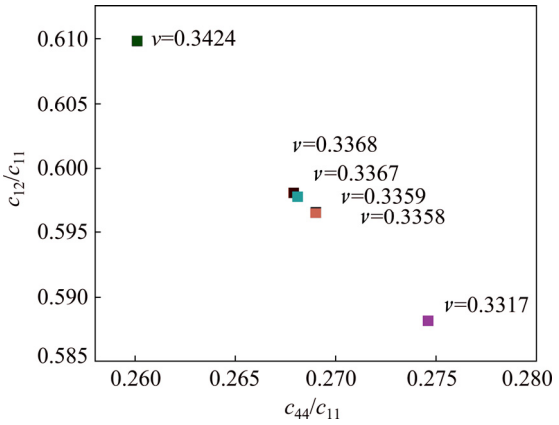

Fig. 7 Blackman diagram and Poisson ratio for alloys shown in Table 3

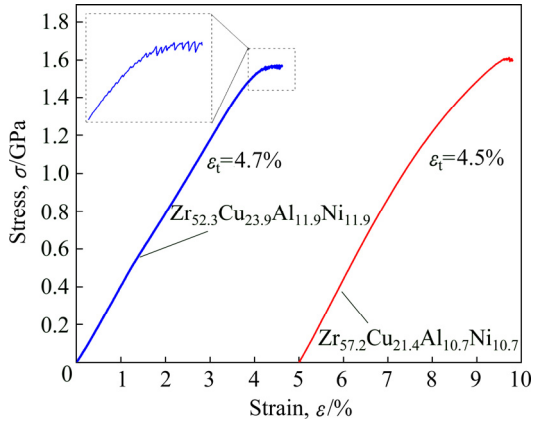

Fig. 8 Compression stress−strain curves for $Zr_{57.2}Cu_{21.4}Al_{10.7}Ni_{10.7}$ and $Zr_{52.3}Cu_{23.9}Al_{11.9}Ni_{11.9}$ bulk metallic glasses

Table 4 Experimentally and theoretically obtained mechanical properties for Zr-based BMG investigated

Chemical composition	σ_y/ GPa	Hardness, H/GPa	ε/%	$E^{1)}$/ GPa	$H^{2)}$/ GPa
$Zr_{57.2}Cu_{21.4}Al_{10.7}Ni_{10.7}$	1.6	4.0	5.2	85	4.2
$Zr_{52.3}Cu_{23.9}Al_{11.9}Ni_{11.9}$	1.57	4.0	5.0	85	4.2

1) $E=50\sigma_y$; 2) $H=2.5\sigma_y$

4 Conclusions

The compact packing and fragility index models were rather useful in designing the chemical composition for the Zr-based alloys with good glass forming ability and ductility. The critical glassy diameter, D_c, for the $Zr_{57.2}Cu_{21.4}Al_{10.7}Ni_{10.7}$ and $Zr_{52.3}Cu_{23.9}Al_{11.9}Ni_{11.9}$ BMG was 3 mm. The good GFA of the investigated alloys was confirmed by the results of the thermally obtained parameters i.e. ΔT_x, T_{rg} and γ. The use of the dense packing and fragility index models did help to predict glass-forming composition in the family alloy investigated. The amount of plastic deformation obtained for both alloys confirmed the predictions of the theoretical calculations, as the percentage of the total experimentally obtained deformation almost tripled the typical values reported for convectional BMGs (≥5%). During the compression test of the glassy samples, an incandescent spark was produced, confirming the increment of temperature, above the liquidus temperature, during the plastic deformation.

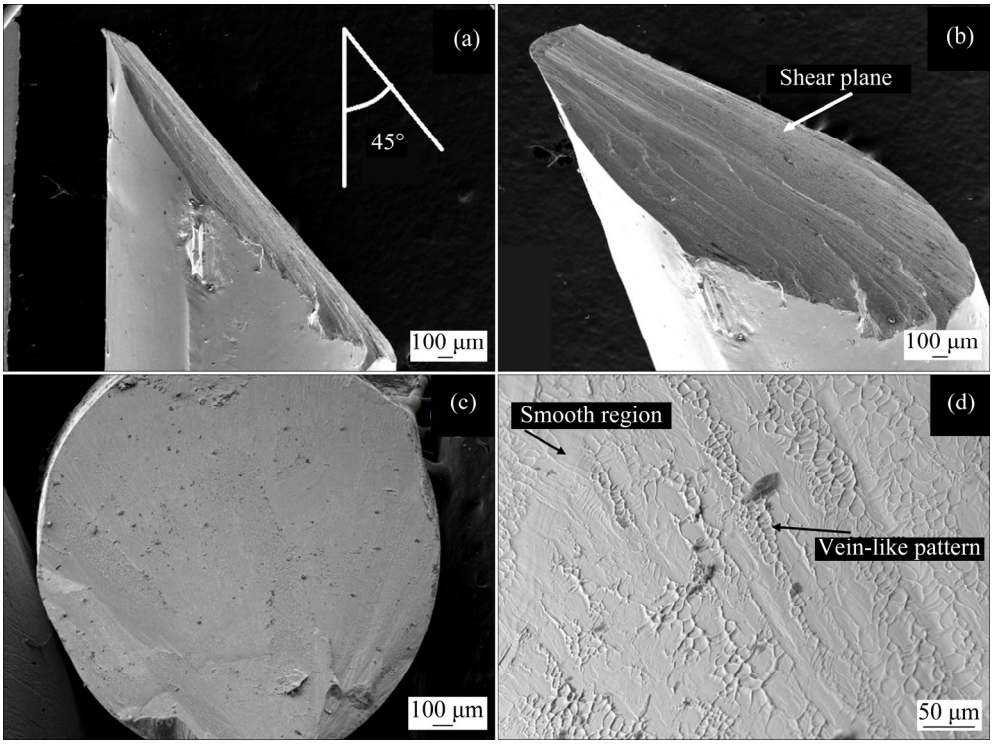

Fig. 9 Fracture morphologies of $Zr_{57.2}Cu_{21.4}Al_{10.7}Ni_{10.7}$: (a) Angle fracture; (b) Shear plane; (c) Cross section; (d) Characteristic pattern

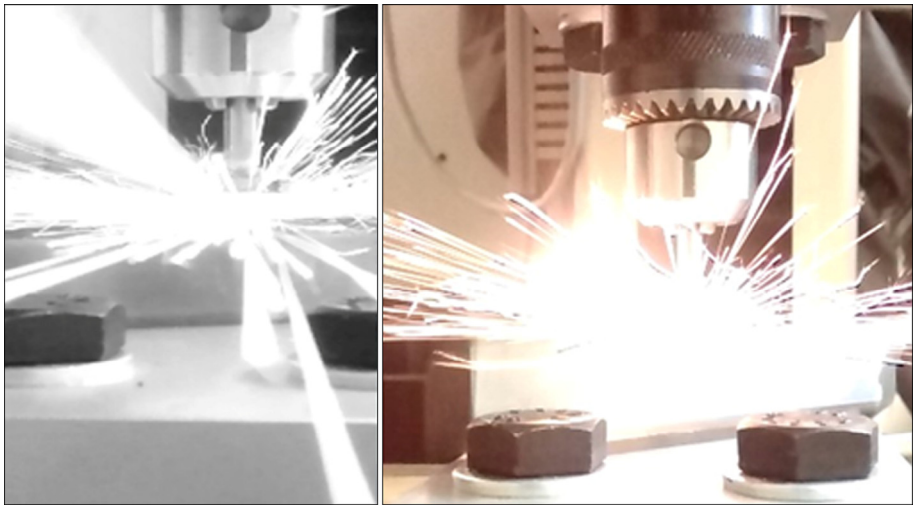

Fig. 10 Incandescent sparks produced after compression test

Acknowledgments

The authors would like to acknowledge the financial support from UNAM-DGAPA-PAPIIT thorough the project 101016. C. E. Borja thanks CONACYT for the 232312 PhD scholarship grant. A. Tejeda-Cruz, C. Flores, J. M. Garcia, F. Garcia, R. Reyes, F. Silvar, C. Ramos, A. Lopez V. and O. Novelo are also acknowledged for their technical support.

References

[1] LI H F, ZHENG Y F, XU F, JIANG J Z. In vitro investigation of novel Ni free Zr-based bulk metallic glasses as potential biomaterials [J]. Materials Letters, 2012, 75: 74−76.

[2] SURYANARAYANA C, INOUE A. Bulk metallic glasses [M]. Florida: CRC Press Taylor & Francis Group, 2011.

[3] NAGASE T, KINOSHITA K, UMAKOSHI Y. Fabrication of Ti−Zr binary wire by arc-melt-type melt-extraction method [J]. Materials Transactions, 2008, 49: 1385−1394.

[4] YUAN Z Z, BAO S L, LU Y, ZHANG D P, YAO L. A new criterion for evaluating the glass-forming ability of bulk glass forming alloys [J]. Journal of Alloys and Compounds, 2008, 459: 251−260.

[5] MIRACLE D B. A structural model for metallic glasses [J]. Nature Materials, 2004, 3: 697−702.

[6] MIRACLE D B. The Influence of efficient atomic packing on the constitution of metallic glasses [J]. Philosophical Magazine, 2003, 83: 2409−2428.

[7] MIRACLE D B. The efficient cluster packing model—An atomic structural model for metallic glasses [J]. Acta Materialia, 2006, 54: 4317−4336.

[8] ANGELL C A. Formation of glasses from liquids and biopolymers [J]. Science, 1995, 267: 1924−1935.

[9] BÖHMER R. NGAI K L, ANGELL C A, PLAZEK D J. Nonexponential relaxations in strong and fragile glass formers [J]. Journal of Chemical Physics, 1993, 99: 4201−4209.

[10] WANG W H. The elastic properties, elastic models and elastic perspectives of metallic glasses [J]. Progress in Materials Science, 2012, 57: 487−656.

[11] PARK E S, NA J H, KIM D H. Correlation between fragility and glass-forming ability/plasticity in metallic glass-forming alloys [J]. Applied Physics Letters, 2007, 91: 031907-1−3.

[12] BORJA C E, FIGUEROA I A, FONSECA J R, LARA G A, VERDUZCO J A. Composition, elastic property and packing efficiency predictions for bulk metallic glasses in binary, ternary and quaternary systems [J]. Materials Research, 2016, 19: 285−294.

[13] LIENHARD IV J H, LIENHARD V J H. A Heat transfer textbook [M]. Third edition. Massachusetts: Phlogiston Press, 2016.

[14] FIGUEROA I A, DAVIES H A, TODD I. Formation of Cu-Hf-Ti bulk metallic glasses [J]. Journal of Alloys and Compounds, 2007, 434: 164−166.

[15] GONZÁLEZ S, FIGUEROA I A, ZHAO H, DAVIES H A, TODD I, ADEVA P. Effect of mischmetal substitution on the glass-forming ability of Mg−Ni−La bulk metallic glasses [J]. Intermetallics, 2009, 17: 968−971.

[16] FIGUEROA I A, DAVIES H A, TODD I, HAWKSWORTH P, VERDUZCO J A. Effect of titanium in Cu-Hf based bulk metallic glasses [J]. Advances in Technology of Materials and Materials Processing Journal, 2006, 8: 146−151.

[17] BORJA C E, FIGUEROA I A, LARA G A, VERDUZCO J A. Glass forming ability and mechanical properties of $Zr_{57.52}Co_{21.24}Al_{9.24}Ag_{12}$ bulk metallic glass [J]. Materials Research, 2015, 19: 86−91.

[18] FIGUEROA I A, CARROL P A, DAVIES H A, JONES H, TODD I. Preparation of Cu-based bulk metallic glasses by suction casting [C]//Proceedings of the Fifth Decennial International Conference on Solidification Processing. Sheffield: University of Sheffield, 2007: 479−482.

[19] CAI A H, XIONG X, LIU Y, AN W K, TAN J Y, PAN Y. Design of new Zr−Al−Ni−Cu bulk metallic glasses [J]. Journal of Alloys and Compounds, 2009, 468: 432−437.

[20] LEDBETTER H, SUDOOK K. Handbook of elastic properties of solids, liquids and gases [M]. Vol. 2. New York: Academic Science, 2001.

[21] SUN B A, WANG W H. The fracture of bulk metallic glasses [J]. Progress in Materials Science, 2015, 74: 211−307.

[22] LEWANDOWSKI J J, GREER A L. Temperature rise at shear bands in metallic glasses [J]. Nature Materials, 2006, 5: 15−18.

ZrCuAlNi 系大块金属玻璃的非晶形成能力、热学和力学性能

C. E. BORJA[1], I. A. FIGUEROA[2], O. LOZADA-FLORES[2],
M. ESTRADA[2], G. A. LARA-RODRÍGUEZ[2], J. A. VERDUZCO[1]

1. Instituto de Investigación en Metalurgia y Materiales,
Universidad Michoacana de San Nicolás de Hidalgo (UMSNH),
Fco. J. Mújica S/N, Col. Felícitas del Río, C.P. 58030, Morelia, Mich., México;
2. Instituto de Investigaciones en Materiales, Universidad Nacional Autónoma de México (UNAM),
Circuito Exterior S/N, Cd. Universitaria, C.P. 04510, Cd. Mx., México

摘　要：分析 ZrCuAlNi 系大块金属玻璃的非晶形成能力、热学和力学性能。运用密实堆积和动态脆性指数模型从理论上确定合金的成分。采用铜模吸铸法在氩气保护下制备圆柱形和圆锥形铸锭。用 X 射线衍射表征圆锥形铸锭以便确定非晶结构。结果表明：两种合金的临界非晶直径为 3 mm。用差示扫描量热法（DSC）分析其热行为，加热速率分别为 0.5、0.67 和 0.83 K/s。γ 参数、过冷液相区 ΔT_x 和约化玻璃转变温度 T_{rg} 等这些实验所得的参数均表明其具有高的非晶形成能力。非晶成分显示其脆性指数为 40。合金的压缩试验采用的应变速率为 0.016 s^{-1}，得到弹性模量约为 83 GPa，总应变约为 5%，屈服强度为 1.6 GPa，硬度为 4 GPa。运用密实堆积和动态脆性指数模拟可以预测 ZrCuAlNi 系合金的非晶形成成分。

关键词：大块金属玻璃；非晶形成能力；脆性指数；堆积率；吸铸

(Edited by Xiang-qun LI)